Chemical Science

ROYAL SOCIETY OF CHEMISTRY

EDGE ARTICLE

View Article Online
View Journal | View Issue

Check for updates

Cite this: *Chem. Sci.*, 2025, **16**, 15446

All publication charges for this article have been paid for by the Royal Society of Chemistry

Received 10th June 2025
Accepted 22nd July 2025

DOI: 10.1039/d5sc04242a

rsc.li/chemical-science

Open Access Article. Published on 24 July 2025. Downloaded on 1/14/2026 11:15:21 PM. This article is licensed under a Creative Commons Attribution-NonCommercial 3.0 Unported Licence.

A simple synthesis of group 2 anthracenides and their use as reducing agents for polypnictogen ligand complexes†

Lukas Adlbert,‡[a] Martin Weber,‡[a] Christoph Riesinger,[a] Michael Seidl[b] and Manfred Scheer *[a]

By using an improved synthetic pathway, the anthracenides of the group 2 metals Ca, Sr, and Ba are straightforwardly accessible for subsequent organometallic syntheses. These highly reactive compounds are slightly soluble in tetrahydrofuran and can be used as synthons for group 2 metal transfer due to the lability of the anthracene substituent. These features were used to explore their reactivity towards the polyphosphorus ligand complexes [Cp*Fe(η^5-P_5)] (Cp* = $C_5(CH_3)_5$) and [Cp*Fe($\eta^{3:1}$-(1-CH_3-2-PPh_2-P_5))], respectively. The resulting products, [Cp*Fe(μ-$\eta^{4:2:1}$-P_5)Mg(thf)$_3$] 0.5 thf (thf = tetrahydrofuran) and [{Cp*Fe(μ-$\eta^{2:2:1}$-(1-CH_3-2-PPh_2-P_5))}$_2$Mg(thf)$_2$]·3 thf, are first examples of molecular magnesium-containing polypnictogenide transition metal complexes without stabilization by N-donor ligands that are soluble in organic N-donor-free solvents. The P_{12} ligand in the latter complex is the first example of a 2,2′-diphosphanyl-substituted decaphosphadihydrofulvalen-shaped structural motif (2,2′-bis(diphenylphosphanyl)-1,1′-dimethyl-3,3′-bipentaphosphole). The complexes [Cp*Fe(μ_3-$\eta^{4:4:1}$-P_5)Sr(thf)$_4$]$_2$·2 thf and [Cp*Fe(μ_3-$\eta^{2:1:1:1:1}$-(1-CH_3-2-PPh_2-P_5))Sr(thf)$_3$]$_2$·2 thf represent the first examples of molecular polypnictogen compounds of strontium that are stable in organic solvents.

Introduction

In recent years, the chemistry of the alkaline earth metals Mg, Ca, Sr, and Ba has experienced a revival.[1–4] While beryllium chemistry has also gained increasing attention, it remains distinct due to its fundamentally different chemical behavior and the challenges associated with its handling, particularly its toxicity.[5–10] Recent studies focus on group 2 metals stabilized by N-donor ligands as in the case of the Mg(I) species [^{Dipp}BDIMg]$_2$ (BDI = β-diketiminate, Dipp = di(*iso*-propyl)phenyl).[11–17] In particular, the chemistry of the heavier metals Ca, Sr, and Ba is less well explored than that of Mg. The activation of heavy group 2 metals is mandatory for synthetic applications due to passivation effects and their high melting and boiling points, which prohibit, for example, the formation of metal mirrors as is commonly done for Na or K. These challenges in working with alkaline earth metals are even more pronounced for the heavier representatives.[18–20] For Mg, different techniques of activation are known, and the use of Grignard reagents, for example, is fairly common in modern laboratory syntheses. A rather unusual form of activation is the formation of magnesium anthracenide (MgA, A = anthracenediide) by heating magnesium turnings in a saturated solution of anthracene in THF (THF = tetrahydrofuran) for a prolonged period with small amounts of MeI added for the initial activation.[21] The formed anthracenide can be directly used as a highly reactive synthon for Mg, forming anthracene upon reduction of a suitable substrate. It is worth mentioning that anthracene is a non-innocent ligand that can influence reactivity and, in some cases, participate in reactions.[22–26] Although its solubility is low and the use of donor solvents such as THF is mandatory, the advantage of MgA as an Mg synthon in organometallic chemistry is its solubility as compared to Mg itself, which prevents reactions from taking place directly on the metal surface.

Anthracenides are also known for the heavier homologs of Mg. However, their synthesis is considered rather challenging as it requires ball milling in mineral oil and large amounts of starting materials, while yielding only poor to moderate amounts of the respective anthracene compounds with low purity.[27] Reasons for this are the higher electron-donating nature of the heavier alkaline earth metals, passivation effects on the metal surface, as well as the decreased solubility and higher reactivity of the formed products.[27] Thus, bulky, electron-donating ligands are usually required to stabilise organometallic compounds of Ca, Sr, and Ba. The need for

[a]*Institute of Inorganic Chemistry, University of Regensburg, Universitätsstr. 31, 93053 Regensburg, Germany. E-mail: Manfred.scheer@chemie.uni-regensburg.de*

[b]*Institute for General, Inorganic and Theoretical Chemistry, University of Innsbruck, Innrain 80-82, 6020 Innsbruck, Austria*

† Electronic supplementary information (ESI) available. CCDC 2453848–2453854. For ESI and crystallographic data in CIF or other electronic format see DOI: https://doi.org/10.1039/d5sc04242a

‡ These authors contributed equally to this work.

© 2025 The Author(s). Published by the Royal Society of Chemistry

Open Access Article. Published on 24 July 2025. Downloaded on 1/14/2026 11:15:21 PM. This article is licensed under a Creative Commons Attribution-NonCommercial 3.0 Unported Licence.

highly sterically demanding ligands also applies to the β-diketiminate ligands required to stabilise the respective Sr or Ba compounds [^{DIPeP}BDISrH]$_2$ (DIPeP = 2,6-di-(*iso*-pently)phenyl) and [^{DIPeP}BDIBaN(SiMe$_3$)$_2$].[11,12] Likewise, the use of 9,10-bis(-trimethylsilyl)anthracene has proved to be an effective strategy to stabilise Ba, highlighting its potential as a supporting ligand for heavier alkaline earth metal complexes.[28] The cleavage of ethers as for instance THF, which are used as solvents, is observed for all alkaline earth anthracenide compounds upon moderate heating, and Sr and Ba compounds slowly form the amides upon dissolution in liquid ammonia.[29]

Due to these challenges, the reactivity of such group 2 metal compounds towards group 15 elements is largely unexplored. In the past, polyphosphides of Ca, Sr, and Ba were only known to exist in the solid state or in liquid ammonia as a solvent.[30–41] Until recently, only four molecular polyphosphides of Mg, soluble in organic solvents, were known: [{^{Dipp}BDIMg}$_2$(μ-η$^{1:1:1:1}$-^{n}Bu$_2$P$_4$)], [{^{Dipp}BDIMg}$_2$(μ-η$^{1:1:1:1}$-^{n}Bu$_2$P$_8$)], [{^{Dipp}BDIMg}$_3$(μ$_3$-η$^{1:1:1:1:1:1}$-P$_7$)], and [As{GaC(SiMe$_3$)$_3$}$_3$-P$_3$Mg(thf)$_3$] (*cf.* Scheme 1).[13,42] Our group reported a supramolecular aggregate of the polyphosphorus ligand complex [Cp*Fe(η^5-P$_5$)] (**1**, Cp* = C$_5$(CH$_3$)$_5$) and the Mg(I) species [^{Dipp}BDIMg]$_2$, as well as novel molecular Ca polyphosphides.[43] Very recently, Harder and co-worker reported novel Mg and Ca polyphosphides (P_4^{2-}, P_7^{3-}, and P_8^{4-}) featuring [^{Dipp}BDIMg] and [(^{DIPeP}BDI)M] (M = Mg, Ca).[44]

No molecular polyphosphides of Sr or Ba are known to date, making Sr diphosphanylsiloxanide [{P$_2$(^{i}Pr$_2$Si)$_2$O}$_2${Sr(dme)$_2$}$_2$] (dme = dimethoxyethane) the only existing molecular diphosphide-like compound of Sr that is soluble in organic solvents.[45] However, all the examples of Mg and Ca possess N-containing β-diketiminate substituents protecting the soluble products from further aggregations. Therefore, the question arose as to how group 2 metals without N-donor ligands would behave as reducing agents and whether more soluble aggregates could be achieved. In this context, we aimed for the development of an improved synthesis of anthracenide reagents (*vide infra*), which proved crucial in generating well-dispersed and reactive group 2 metal species. This enhanced synthetic control allowed us to explore new polypnictogen reactivity and access molecular complexes that were previously inaccessible due to solubility and aggregation challenges.

For these investigations, pentaphosphaferrocene [Cp*Fe(η^5-P$_5$)] (**1**) and its functionalized derivative [Cp*Fe(η$^{3:1}$-(1-CH$_3$-2-PPh$_2$-P$_5$))][46] (**2**) were chosen. The redox chemistry of **1** was first investigated by electrochemical studies, which revealed its ECEC processes, *i.e.* a reaction cascade involving electrochemical oxidation or reduction, chemical reaction, which in this particular case is a dimerisation after oxidation and reduction, electrochemical reduction or oxidation of the formed dimer, and another chemical reaction, in this case reformation of the original monomer in a so-called square scheme.[47] Our group was able to prove the identity of these products by reducing **1** with potassium to [K(dme)$_2$K(dme)][{Cp*Fe$_2$(μ-η$^{4:4}$-P$_{10}$)] and oxidising it with thianthrenium salts to [{Cp*Fe$_2$(μ-η$^{4:4}$-P$_{10}$)][SbF$_6$]$_2$.[48] Furthermore, the dianionic species [K(dme)K(di-benzo-18-crown-6)][Cp*Fe(η^4-P$_5$)] was identified. When other reagents for the reduction of **1**, such as [(Cp*Fe)(Cp‴Co)(μ-η$^{5:4}$-P$_5$)], [(DIP$_2$pyr)SmI(thf)$_3$] (DIP$_2$pyr = 2,5-bis{*N*-(2,6-diisopropylphenyl)-iminomethyl}pyrrolyl) or carbon nucleophiles (*e.g.*, RLi, R = Me, ^{t}Bu), as well as [(^{Dipp}BDI-Mg(CH$_3$))$_2$] were used, products with similar structures involving a η^4-coordination mode and one phosphorus atom bent out of the plane were obtained.[43,49–51]

Herein we report on an improved synthetic pathway to the heavier group 2 anthracenides and their use as reducing agents in polyphosphorus ligand complex chemistry.

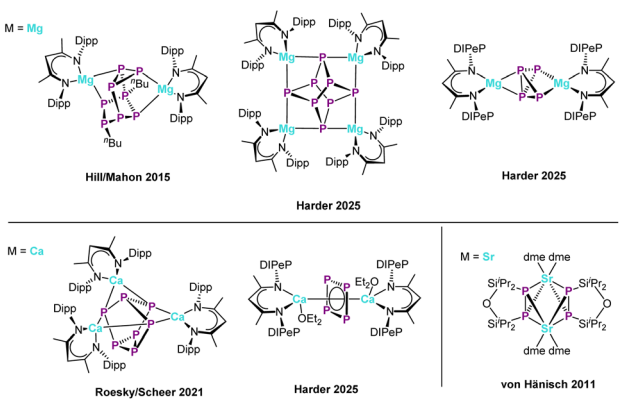

Scheme 1 Selected literature examples of molecular polyphosphides of alkaline earth metals (M = Mg–Ca) that are soluble in organic solvents, beside the poorly soluble [(BDI)Mg]$_4$(P$_8$) and the structurally distinct diphosphide-like compound of Sr (DIPeP = 2,6-di-(*iso*-pentyl)phenyl, Dipp = di(*iso*-propyl)phenyl, dme = dimethoxyethane, Et = ethyl, ^{i}Pr = *iso*-propyl, thf = tetrahydrofuran).

Results and discussion

Synthesis of alkaline earth metal anthracenides

From the existing literature on the synthesis of the alkaline earth metal anthracenides, it is evident that the activation of the group 2 metal and its fine dispersion as a powder are crucial steps for a feasible synthesis route.[27] Ball milling of alkaline earth metals suspended in mineral oils introduces multiple possible sources of contamination while reducing the yields as well as the purity of the final products. In contrast, dissolving the metal in liquid ammonia appears to be a relatively easy way to convert lumps of Ca, Sr, or Ba into a powder or a microporous solid. Thus, a small amount of ammonia was condensed onto the metal and removed after most of the metal was dissolved, as described by Westerhausen for the activation of the heavier group 2 elements for subsequent syntheses of heavy alkaline earth metal Grignard reagents.[19] This also eliminates the necessity of further activating the finely dispersed metal in solution with a halide activator such as MeI (as done *e.g.* by Bönnemann *et al*),[27] provided that not even trace amounts of water or oxygen come into contact with the metal before the anthracenide begins to form (visible by vibrant colors, *vide infra*). Therefore, a synthesis route (Scheme 2) was designed in which not even standard inert gas from the Schlenk line was

© 2025 The Author(s). Published by the Royal Society of Chemistry

Open Access Article. Published on 24 July 2025. Downloaded on 1/14/2026 11:15:21 PM.
This article is licensed under a Creative Commons Attribution-NonCommercial 3.0 Unported Licence.

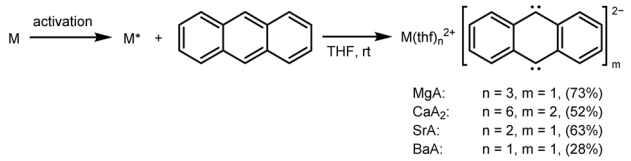

Scheme 2 Generalised activation (by sonication (Mg) and dissolution in liquid ammonia (Ca–Ba), respectively) of the alkaline earth metal and reaction pathway to alkaline earth metal anthracenides $M(thf)_nA_m$ featuring an improved synthetic approach (M = Mg ($n = 3$, $m = 1$), Ca ($n = 6$, $m = 2$), Sr ($n = 2$, $m = 1$), Ba ($n = 1$, $m = 1$)). Isolated yields are given in parentheses.

applied, but where THF and anthracene were sublimed and condensed, respectively, and added under high vacuum (*cf.* ESI†).

After metal activation by sonication (Mg) and dissolution in liquid ammonia with the subsequent removing of NH_3 (Ca–Ba), respectively, and the addition of anthracene and a stirring bar, THF (dried and stored over potassium mirror/benzophenone) is condensed onto the solid mixture while it is cooled in a liquid nitrogen bath. The valve is closed while the flask is still under vacuum and allowed to warm to room temperature. For Sr and Ba, the reaction initiates within one hour of vigorous stirring. The onset of the reaction is indicated by a color change of the reaction mixture (intense color of the suspension: violet for Sr, dark blue for Ba). If no color change is observed within the first hour, the reaction mixture (still under vacuum) should be subjected to an ultrasonic bath to facilitate activation. At this point, dry argon is carefully added to the flask. After all metal powder is consumed, the reaction is considered complete, and the liquid is decanted. The remaining powder is washed three times with cold *n*-pentane, yielding intensely colored, fine, homogeneous powders (MgA 73%, SrA 63%, BaA 28%), comparable in appearance to those obtained in the initial literature procedure.[27]

For Ca, the activation proved to be less reliable, and the synthesis of CaA is particularly challenging due to the possible formation of the dianthracenide species CaA_2. Therefore, the dianthracenide was synthesised deliberately following literature procedures.[27] Additionally, a small amount of MeI was added to the THF suspension of ammonia-activated calcium and anthracene to assist the first step of the reaction. Nevertheless, the reaction still proceeded slowly and required prolonged activation in an ultrasonic bath. During the reaction between Ca and anthracene, the color of the solution changed from brown to green, producing a brownish-gray powder. Upon washing with *n*-pentane, drying under vacuum, and isolation (52%), the powder turned deep violet, which corresponds to the reported color of CaA_2.[27] In contrast, CaA is described as having a brownish-orange color.[27] The refined anthracenide synthesis was not only critical for obtaining well-defined group 2 anthracenide complexes, but also served as a key enabling step for subsequent reactivity studies. The improved solubility and reactivity control allowed for cleaner reduction conditions and better molecular dispersion of the metal centers, which proved essential for accessing the novel polypnictogen complexes reported in the following. Without this optimised synthetic route, the formation and isolation of the structurally characterised molecular polypnictides would have been significantly hindered by poor solubility, aggregation, or decomposition pathways.

Reactivity of alkaline earth metal anthracenides towards pentaphosphaferrocene

In order to use the anthracenides of Mg, Ca, Sr, and Ba as reducing agents towards pentaphosphaferrocene, two equivalents of the respective reductant are mixed with crystalline **1** in a dry Schlenk flask. The flask is then cooled in a bath of liquid nitrogen. THF, stored over a potassium mirror, is directly condensed onto the solid reaction mixture. While the reaction mixture is slowly warmed to room temperature, the flask is shaken vigorously to ensure thorough mixing. The reaction initiates immediately upon melting of the solvent, as evidenced by the appearance of a brown coloration of the mixture. After stirring the resulting brown suspension at room temperature for five minutes, the solids are allowed to settle and the clear, dark brown solution is decanted into another flask. Crystalline products as thf adducts form upon storing the solutions at −30 °C over a period of up to one week.

By using the anthracene compounds of Mg and Sr, the compounds $[Cp^*Fe(\mu\text{-}\eta^{4:2:1}\text{-}P_5)Mg(thf)_3]\cdot 0.5$ thf (**3**, 33%, Scheme 3) and $[Cp^*Fe(\mu_3\text{-}\eta^{4:4:1}\text{-}P_5)Sr(thf)_4]_2 \cdot 2$ thf (**4**, 56%) were isolated and fully characterized. Complex **3** represents the first example of a molecular, transition metal-stabilised alkaline earth polyphosphide without an N-donor ligand that is already soluble in organic ethereal solvents (*e.g.* THF), and complex **4** is indeed the first molecular strontium polyphosphide exhibiting this property. Pentaphosphaferrocene **1** reacted with both

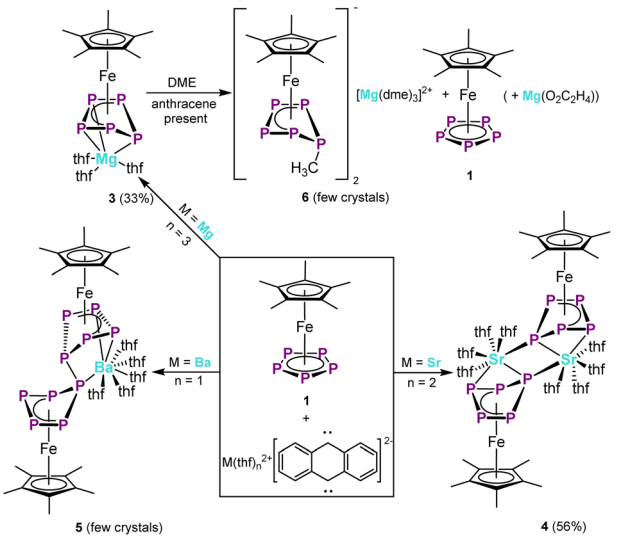

Scheme 3 Reaction of **1** with the alkaline earth metal anthracenides $M(thf)_nA$ (M = Mg ($n = 3$), Sr ($n = 2$), Ba ($n = 1$)). All reactions were performed by condensing THF onto the mixture of solid starting materials, cooled with a liquid nitrogen bath, and warming to room temperature. Isolated yields are given in parentheses.

© 2025 The Author(s). Published by the Royal Society of Chemistry

Open Access Article. Published on 24 July 2025. Downloaded on 1/14/2026 11:15:21 PM. This article is licensed under a Creative Commons Attribution-NonCommercial 3.0 Unported Licence.

[BaA(thf)] and [$CaA_2(thf)_6$], as evidenced by a distinct color change and the absence of signals for **1** in the ^{31}P NMR spectra of the respective reaction solutions. Unfortunately, no product could be isolated or identified from the reaction with [$CaA_2(thf)_6$]. The ^{31}P NMR spectra of the reaction mixtures involving [Ba(thf)A] show an extremely broadened AMM′XX′ spin system, consistent with the expected twofold reduction product of **1** (*vide infra*, most likely structured like **3**). If the solution is stored at room temperature for more than four hours, the signals disappear, and the color of the solution changes to a brighter brown. The same behavior is observed at 0 °C over two to three days or storing the solution at −30 °C over one to two weeks, while maintaining temperatures below 0 °C throughout the storage time. In the reaction with slightly less than two equivalents of [Ba(thf)A] and handling the reaction mixture at −10 °C, a few crystals of [{Cp*Fe}$_2$(μ_3-$\eta^{4:4:2:1}$-P_{10})Ba(thf)$_5$]·0.5 thf (**5**, Scheme 3), suitable for a tentative X-ray structure determination, were obtained after storing the solution at −30 °C for two weeks. It confirmed the connectivity of **5** featuring a P_{10} ligand framework, coordinated by one Ba atom as depicted in Scheme 3 (*cf.* ESI†). Both compounds **3** and **4** (Scheme 3) show an AMM′XX′ spin system in their ^{31}P NMR spectra, consistent with the C_S-symmetric P5 ligand in an envelope conformation (P_A = P1, $P_{MM'}$ = P3/P4, $P_{XX'}$ = P2/P5; P1–P5 as revealed by its X-ray structure in Fig. 1 (left)). In contrast to the 1,3-bisketiminate-stabilised magnesium compound [(^{Dipp}BDI-Mg)$_2$(μ-$\eta^{4:2:1}$-P_5)(FeCp*)],[43] **3** does not exhibit any dynamic process associated with a tumbling of the magnesium atom over the *cyclo*-P_5 ligand. The signals of **4** are slightly broadened as compared to **3**, but still resolved well enough for iterative fitting and simulation of the spectrum.

The chemical shifts of the individual P atoms resemble those observed for [K(dme)K(dibenzo-18-crown-6)][Cp*Fe(η^4-P_5)], yet with systematic trends for the different alkaline-earth metals.[48] Due to the higher basicity of Sr, the multiplet of the A resonance is significantly shifted downfield.[48] The relatively strong downfield shift of the MM′ multiplet in the ^{31}P NMR spectrum of **3** to $\delta = 50$ ppm, compared to −3 ppm for the respective multiplet in the spectrum of **4**, can be explained by stronger coordination of the Mg atom to the respective phosphorus atoms in comparison to the Sr compound **4**.

The solid-state structure of **3** (Fig. 1, left) confirms the existence of a [Cp*FeP_5]$^{2-}$ moiety, with the Mg atom coordinating to the phosphorus atom that is bent out of the plane (P1), as well as to the two opposite P atoms (P3 and P4). The fact that the Mg–P1 bond (2.5624(8) Å) is close to the sum of their covalent radii (2.50 Å)[52] and significantly shorter than the Mg–P3 (2.7788(8) Å) and Mg–P4 (2.8393(8) Å) bonds suggests a stronger coordination of Mg to P1, as confirmed by the chemical shifts of the respective signals in the ^{31}P NMR spectrum of **3** (*vide supra*). The distance of the Mg atom to the centroid of the plane formed by the atoms P2, P3, P4, and P5 is 2.4380(6) Å. The bond lengths and angles of the [Cp*FeP_5]$^{2-}$ moiety in **3** and **4** are similar to those observed in related complexes, such as [K(dme)K(dibenzo-18-crown-6)][Cp*Fe(η^4-P_5)].[48]

In contrast to **3**, **4** crystallises as a dimer where two Sr(thf)$_4$ dications are bridged by two [Cp*FeP_5]$^{2-}$ anions. The bond lengths of Sr to P1 (3.0793(7) Å) and to the P1 atom of the second moiety in the dimeric solid-state structure of **4** (3.1175(7) Å) differ by only 0.038 Å and are comparable to the Sr–P bond lengths in [{P_2(^{i}Pr$_2$Si)$_2$O}$_2${Sr(dme)$_2$}$_2$] (3.1086(11) Å and 3.1271(11) Å).[45] The distance of the Sr atoms to the mean plane of the *cyclo*-P_5 ligand in **4** amounts to 3.0683(4) Å. Both the Sr⋯Sr distance (5.1062(4) Å) and the P1⋯P1′ distance (3.5110(14) Å) are too large for significant Sr⋯Sr or P⋯P interactions.

It was also tested whether **1** could be reduced with alkaline-earth metals itself, with and without small amounts of anthracene present in the reaction mixture. Therefore, the metals were first activated using liquid ammonia, as described above. After months of stirring the reaction mixture together with **1**, a dark, oily residue was observed for the Sr reaction (only when anthracene was present), while no reaction occurred with Mg, Ca, and Ba. Therefore, the reduction potential of the respective M(thf)$_n$A is needed to achieve the reduction step efficiently.

While trying to improve the crystallised yields of **3**, DME was used as a solvent for extracting the crude reaction mixture. Surprisingly, a color change was observed and the ^{31}P NMR spectrum of the reaction solution revealed a different reaction product as compared to **3**, along with the starting material **1** in a 1 : 1 ratio. After X-ray diffraction experiments of some crystals obtained from this solution, the reaction product was identified as [Cp*Fe(η^4-P_5CH_3)]$_2$[Mg(dme)$_3$]·dme (**6**, Scheme 3). The formation of **6** and **1** in a 1 : 1 ratio can be explained by a disproportionation reaction and ether cleavage of DME. In the ^{31}P NMR spectrum of **6**, the chemical shifts and the coupling constants of the AMM′XX′ spin system are identical to those of [Cp*Fe(η^4-P_5CH_3)]$^-$, the product of the nucleophilic methylation of **1** with MeLi.[49] Since the methyl groups are cleaved from the solvent, we assume that magnesium ethylenglycoxide must be formed to balance the reaction equation (Scheme 3). Unfortunately, analytical evidence for this species remains elusive. Repeating the experiment by dissolving pure **3** in neat

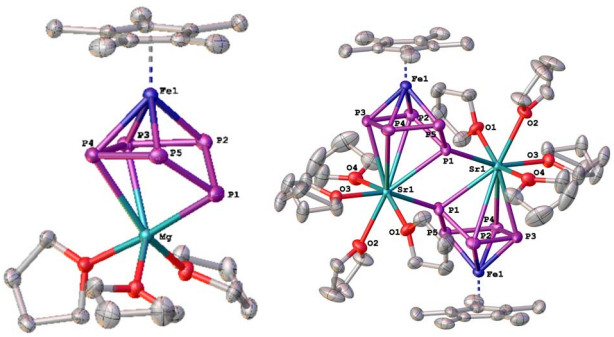

Fig. 1 Molecular structures of **3** (left) and **4** (right) in the solid state. Selected bond lengths of **3**: Fe1–P4 2.3124(5), Fe1–P5 2.2587(5), Fe1–P3 2.2982(5), Fe1–P2 2.2624(5), P4–P5 2.2173(7), P4–P3 2.1713(7), P4–Mg 2.8393(8), P5–P1 2.1762(7), P5–Mg 3.1617(8), P3–P2 2.2229(7), P3–Mg 2.7788(8), P1–P2 2.1771(7), P1–Mg 2.5624(8), P2–Mg 3.0746(8). Selected bond lengths of **4**: Sr1–P2 3.4128(8), Sr1–P1′ 3.1175(7), Sr1–P1 3.0793(7), Sr1–P4 3.7466(8), Sr1–P3 3.1772(7), Fe1–P5 2.2719(8), Fe1–P2 2.2825(7), Fe1–P4 3.2221(8), Fe1–P3 2.2901(8), P5–P1 2.1625(9), P5–P4 2.1971(10), P2–P1 2.1731(11), P2–P3 2.2164(11), P4–P3 2.1488(13).

Open Access Article. Published on 24 July 2025. Downloaded on 1/14/2026 11:15:21 PM. This article is licensed under a Creative Commons Attribution-NonCommercial 3.0 Unported Licence.

DME, in the absence of anthracene, did not result in an ether cleavage.

Reactivity of alkaline earth metal anthracenides towards [Cp*Fe($\eta^{3:1}$-(1-CH_3-2-PPh_2-P_5))]

The cyclic voltammogram of [Cp*Fe($\eta^{3:1}$-(1-CH_3-2-PPh_2-P_5))][46] (**2**) reveals a behavior similar to the one known for **1**,[47] but with lower reduction and oxidation potentials: both the oxidation and reduction are chemically irreversible one electron processes (Fig. 2). The chemical and electrochemical behavior of the resulting 17 valence-electron (VE) oxidation product $[\mathbf{2}]^+$ and the 19 VE reduction product $[\mathbf{2}]^-$ are best described as two ECEC (**e**lectron transfer, **c**hemical Reaction, **e**lectron transfer, chemical Reaction) processes (*vide supra*): After the one-electron oxidation at peak A (peak potential $E_p^{ox,2} = 529$ mV, Fig. 2) of **2** to $[\mathbf{2}]^+$, dimerisation of the 17 VE complex to $[\mathbf{2}]_2^{2+}$ occurs too rapidly to detect a directly associated, cathodic counterpeak for back-reduction of $[\mathbf{2}]^+$ to **2**, even at a scan rate of 1000 mV s^{-1}. However, the dimer $[\mathbf{2}]_2^{2+}$ is then reduced back to **2** on traversing wave B at $E_p^{red,[2]2+} = -19$ mV, Fig. 2). The same overall behavior applies to the respective one-electron reduction at $E_p^{red,2} = -1600$ mV (peak C in Fig. 2) and the oxidation of the resulting dimer $[\mathbf{2}]_2^{2-}$, observed as peak D at $E_p^{ox,[2]2-} = 915$ mV).

When complex **2** is reacted with MgA and SrA, respectively, under the same experimental conditions as used for **1** (*vide supra*), crystals of [{Cp*Fe(μ-$\eta^{2:2:1}$-(1-CH_3-2-PPh_2-P_5))}$_2$-Mg(thf)$_2$]·3 thf (**7**, 30%) and [Cp*Fe(μ_3-$\eta^{2:1:1:1:1}$-(1-CH_3-2-PPh_2-P_5))Sr(thf)$_3$]$_2$·2 thf (**8**, 28%) are obtained by storing the respective THF solutions at −30 °C for one week (Scheme 4).

The solid-state structures of **7** and **8** (Fig. 3 and 4) show a central metallo-nortricyclane structural motif. In **7**, a new P–P bond is formed between two units of the one-electron reduced **2**. The resulting P_{12}^{2-} ligand can be described as a 2,2′-bis(diphenylphosphanyl)-1,1′-dimethyl-3,3′-bipentaphosphole and represents the first example of this 2,2′-diphosphanyl-substituted decaphosphadihydrofulvalen-shaped structural motif of a homoatomic polyphosphorus P_{12} moiety (Fig. 3, right). The Mg–P bonds in **7** differ by *ca.* 0.5 Å (2.574(3) Å and 3.042(2) Å). The length of the newly formed bond P1–P1 (2.224(3) Å) is similar to the other P–P bonds in **7**. The structure of the {Cp*Fe}$_2$(μ-P_{12}) framework in **7** is identical to that postulated for $[\mathbf{2}]_2^{2-}$, the product of the reductive ECEC process, as deduced from the cyclic voltammetry measurements (*vide supra*) and the analogy with that of pentaphosphaferrocene itself.

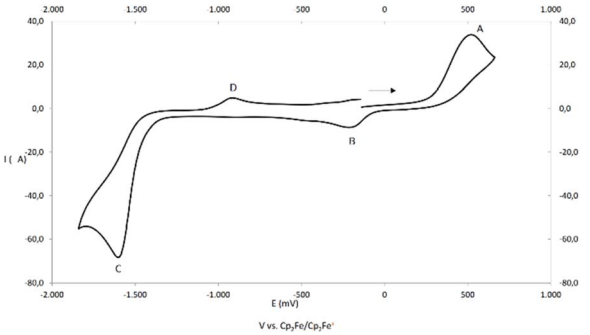

Fig. 2 Cyclic voltammogram of **2** in dichloromethane.

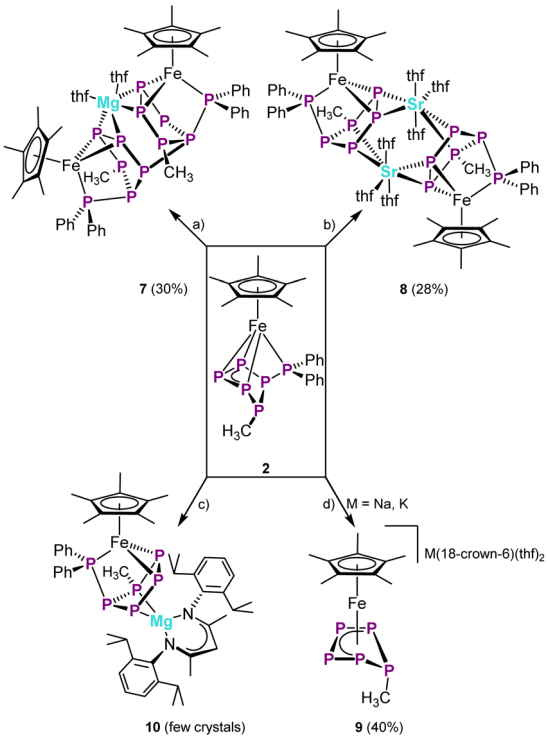

Scheme 4 Reaction of **2** with several reducing agents: (a) with one or two equivalents of MgA in THF at approximately −108 °C (THF condensed and frozen onto the solid starting materials and slowly melting), (b) with one or two equivalents of SrA in THF at *ca.* −108 °C (THF condensed and frozen onto the solid starting materials and slowly melting), (c) with [(^{Dipp}BDI)Mg]$_2$ at −80 °C in toluene, and (d) over potassium or sodium mirror in THF at room temperature. Isolated yields are given in parentheses.

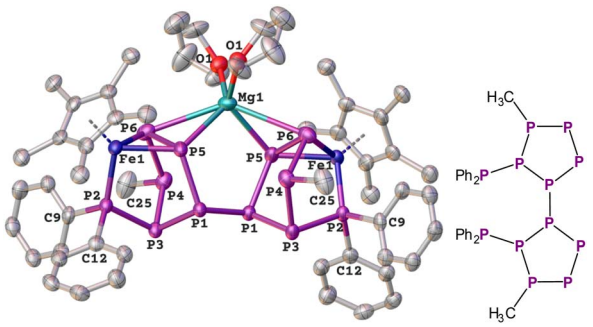

Fig. 3 Molecular structure of **7** in the solid state (left) and schematic depiction of the novel (2,2′-bis(diphenylphosphanyl)-1,1′-dimethyl-3,3′-bipentaphosphole) ligand for easier understanding (right). Hydrogen atoms are omitted for clarity. Selected bond lengths: Fe1–P2 2.1472(18), Fe1–P5 2.2599(17), Fe1–P6 2.260(2), P1–P1′ 2.224(3), P1–P3 2.201(2), P1–P5 2.226(2), P2–P3 2.253(2), P2–C9 1.846(7), P2–C12 1.847(7), P3–P4 2.188(3), P4–P6 2.226(3), P4–C25 1.850(8), P5–P6 2.198(3), P5–Mg1 2.574(3), P6–Mg1 3.042(2).

© 2025 The Author(s). Published by the Royal Society of Chemistry

Open Access Article. Published on 24 July 2025. Downloaded on 1/14/2026 11:15:21 PM.
This article is licensed under a Creative Commons Attribution-NonCommercial 3.0 Unported Licence.

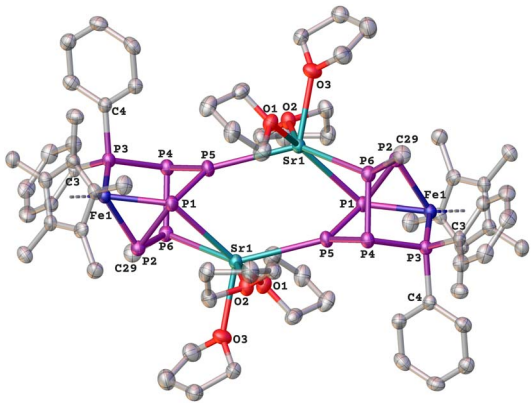

Fig. 4 Molecular structure of **8** in the solid state. Hydrogen atoms are omitted for clarity. Selected bond lengths: Sr1–Sr1′ 4.3804(7), Sr1–P1′ 3.1202(11), Sr1–P2′ 3.2806(11), Sr1–P5′ 3.2418(12), Sr1–P5 3.1088(11), Sr1–P6′ 3.1696(12), Sr1–O1 2.523(3), Sr1–O2 2.562(3), Sr1–O3 2.538(3), Fe1–P1 2.2641(12), Fe1–P2 2.2781(12), Fe1–P3 2.1399(12), P1–P2 2.2040(15), P1–P5 2.2247(15), P2–P6 2.2294(16), P3–P4 2.2757(15), P3–C3 1.844(4), P3–C4 1.847(4), P4–P5 2.1684(16), P4–P6 2.1852(16), P6–C29 1.856(5).

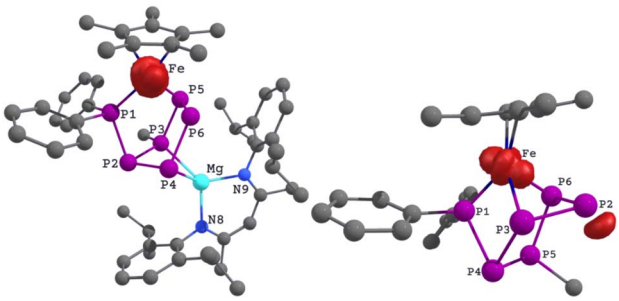

Fig. 5 Calculated spin density for **10** (left) and its radical anion fragment $[Cp^*Fe(\eta^{1:1:1}\text{-}(1\text{-}CH_3\text{-}2\text{-}PPh_2\text{-}P_5))]^-$ (right). Hydrogen atoms are omitted for clarity. (Triplet; BP86-D4/def2-SVP; isovalue = 0.012 a. u.).

In contrast, the solid-state structure of **8** (Fig. 4) is best described as a dimer of the dianion of **2**, with strontium coordinating two units of the doubly reduced complex. The central structural motif is similar to the one in **7**, except that no P–P bond exists between the two units. Using MgA as reducing agent for **2** has so far produced only the P_{12} containing ligand in **7**. SrA appears to be the more powerful reducing agent, resulting in the two-electron reduction of **2**, thereby preventing P–P bond formation. A ^{31}P NMR study was conducted to investigate the reducing strength of the anthracenediides towards **2** in more detail. With less than one equivalent of the anthracenediides the ^{31}P NMR spectra of the reaction solutions show both **2** and the dimer of the respective one-electron reduced product, *i.e.* $[\mathbf{2}]_2^{2-}$. When at least two equivalents of the respective anthracenediide are used, the ^{31}P NMR spectra of the reaction solutions show **2** and **7** in a 1 : 1.8 ratio for MgA, whereas only signals attributed to **8** are observed when using SrA (*cf.* Fig. S17 and S20†). Thus, the reducing power of MgA is only sufficient to form **7** in an equilibrium with the starting material, while the reducing power of SrA is sufficient to reduce **2** entirely to the doubly reduced **8**.

Since the reduction products of **1** with alkali metal mirrors are already known, the use of sodium and potassium mirrors for the reduction of **2** was tested. After several attempts, crystals of $[Cp^*Fe(\eta^4\text{-}(P_5CH_3))][K(18\text{-crown-6})(thf)_2]$ (**9**) were obtained as the only product (Scheme 3). This suggests that the reduction of **2** with alkali metals leads to its conversion by extruding the PPh_2 group, yielding $[Cp^*Fe(\eta^4\text{-}P_5CH_3)]^-$ as the ultimate product. In contrast, the anthracene compounds, although highly reactive, do not show any signs of decomposition of the starting material **2**.

To investigate the influence of sterically demanding N-donor ligands, **2** was reacted with the Mg(I) dimer $[(^{Dipp}BDI)Mg]_2$. Upon reduction of **2** with $[(^{Dipp}BDI)Mg]_2$ in toluene at room temperature, extraction with *n*-pentane, and storing the orange-brown solution at −30 °C for four months after decanting, few orange crystals of $[Cp^*Fe\{\mu\text{-}\eta^{2:1:1:1}\text{-}(1\text{-}CH_3\text{-}2\text{-}PPh_2\text{-}P_5)\}Mg(^{Dipp}BDI)]^\bullet \cdot 0.5$ pentane (**10**) were obtained, alongside amorphous brown solids and a brown oil. The $^{31}P\{^1H\}$ NMR spectrum of the mother liquor shows a complex product mixture which precludes structural assignment and from which no other pure product could be isolated in spite of numerous attempts. Compound **10** features a metallo-nortricyclane structural motif similar to that of **7** and **8**. The formation of **10** corresponds to a single-electron reduction of **2** to $[Cp^*Fe(\eta^{1:1:1}\text{-}(1\text{-}CH_3\text{-}2\text{-}PPh_2\text{-}P_5))]^-$, the product postulated by *cyclo*-voltammetric investigation. This species is not expected to be stable and should dimerise to form the above-mentioned P_{12}^{2-} dianion. However, in the case of **10**, dimerisation is not possible due to the more covalent nature of the $^{Dipp}BDIMg$–P bond and the steric shielding provided by the β-diketiminate ligand and the Dipp-groups of the ligand. Due to the small quantity of **10** in a complex reaction mixture, its isolation and full spectroscopic characterisation have not yet been successful. Density functional theory (DFT) calculations (*cf.* ESI†) on the spin density distribution of **10** and its theoretical fragment $[Cp^*Fe(\eta^{1:1:1}\text{-}(1\text{-}CH_3\text{-}2\text{-}PPh_2\text{-}P_5))]^-$ (*vide supra*) revealed that in **10**, the spin density is almost exclusively located at the Fe atom (99%), whereas in the radical anion fragment, the spin density is mainly distributed between the Fe atom (57%) and the P5 atom (30%), as visualised in Fig. 5. Based on this spin density distribution, the dimerisation to form the P_{12}^{2-} dianion $[Cp^*Fe(\eta^{1:1:1}\text{-}(1\text{-}CH_3\text{-}2\text{-}PPh_2\text{-}P_5))]_2^{2-}$ was modeled by connecting two radical P2 centers (cf. Fig. 5 right). In comparison, DFT calculations of the bond dissociation energy show that the cleavage of the Mg–P bond in **10** to yield $[Cp^*Fe(\eta^{1:1:1}\text{-}(1\text{-}CH_3\text{-}2\text{-}PPh_2\text{-}P_5))]^-$ and $[Mg(DippBDI)]^+$ requires $\Delta G = 589.8$ kJ mol^{-1}, whereas the dissociation of the theoretical P_{12}^{2-} dianion to two $[Cp^*Fe(\eta^{1:1:1}\text{-}(1\text{-}CH_3\text{-}2\text{-}PPh_2\text{-}P_5))]^-$ fragments accounts for $\Delta G = -148.3$ kJ mol^{-1}. Thus, the formation of **10** is strongly favored over the formation of the P_{12}^{2-} dianion, which is in line with the experimental observations.

Conclusions

By activating the alkaline-earth metals Ca, Sr and Ba with liquid ammonia, an improved and simple synthesis of the

Open Access Article. Published on 24 July 2025. Downloaded on 1/14/2026 11:15:21 PM. This article is licensed under a Creative Commons Attribution-NonCommercial 3.0 Unported Licence.

corresponding anthracenides of these metals was developed. Since this synthetic pathway does not rely on ball milling under mineral oil or large amounts of starting materials, it can readily be performed using standard Schlenk techniques.

The high reducing power of these anthracenides and –diides without sterically demanding and stabilizing N-donor ligands was then demonstrated and exploited in their reactions with pentaphosphaferrocene (**1**) and [Cp*Fe($\eta^{3:1}$-(1-CH_3-2-PPh_2-P_5))] (**2**), respectively. Starting from [Cp*Fe(η^5-P_5)] (**1**) and the anthracene compound of Mg, the complex [Cp*Fe(μ-$\eta^{4:2:1}$-P_5)$Mg(thf)_3$]·0.5 thf (**3**) was obtained and fully characterised. It represents the first molecular polyphosphide transition metal complex of magnesium without N-donor ligands that is soluble in ethereal solvents (*e.g.* THF). Reaction of **1** with the THF solvate of Sr anthracenediide yields [Cp*Fe(μ_3-$\eta^{4:4:1}$-P_5)$Sr(thf)_4]_2$·2 thf (**4**), the first molecular polyphosphide compound of strontium that is stable in organic solvents. Although the dianthracenide of Ca reacts with **1**, as indicated by a color change of the reaction mixture, no products from this reaction could be isolated or identified. With the anthracenediide of Ba, the formation of an extremely temperature-sensitive product was observed in the ^{31}P NMR spectra of freshly prepared reaction solutions. This short-lived product could not be isolated, but trace amounts of [{Cp*Fe}$_2$(μ_3-$\eta^{4:4:2:1}$-P_{10})$Ba(thf)_5$]·0.5 thf (**5**), the first molecular polyphosphide compound of barium, were isolated when less than two equivalents of BaA were used in the reaction.

The anthracenides of Mg and Sr also proved to be valuable in exploring the redox chemistry of the complex [Cp*Fe($\eta^{3:1}$-(1-CH_3-2-PPh_2-P_5))] (**2**). Alkali metals Na and K proved to be too harsh as reducing agents for **2**, leading to decomposition of the starting material. However, the anthracenide of Mg successfully achieved a single electron reduction of **2** with subsequent dimerisation of the as-formed anion [**2**]$^-$ through P–P bond formation to afford [{Cp*Fe(μ-$\eta^{2:2:1}$-(1-CH_3-2-PPh_2-P_5))}$_2$-$Mg(thf)_2$]·3 thf (**7**). Complex **7** contains an unprecedented, functionalised 2,2′-bis(diphenylphosphanyl)-1,1′-dimethyl-3,3′-bipentaphosphole ligand. A two-electron reduction to [Cp*Fe(μ_3-$\eta^{2:1:1:1:1}$-(1-CH_3-2-PPh_2-P_5))$Sr(thf)_3]_2$·2 thf (**8**) was observed when the anthracenediide of Sr was used for the reduction of **2**. Reduction with [(^{Dipp}BDI)Mg]$_2$ produced mixtures of different products, of which only [Cp*Fe{μ-$\eta^{2:1:1:1}$-(1-CH_3-2-PPh_2-P_5)}Mg(^{Dipp}BDI)]$^\bullet$ (**10**) could be identified by X-ray diffraction analysis. This product represents the product of a one-electron reduction of **2** without subsequent dimerisation, which is thwarted by the sterically demanding N-donor ligand of [(^{Dipp}BDI)Mg]$_2$. A comparison of the reactivity of **2** towards [Mg(η^2-$C_{14}H_{10}$)$(thf)_3$] and [(^{Dipp}BDI)Mg]$_2$ shows that stabilisation of Mg by bulky donor ligands is not required to form stable polyphosphides in solution. Bulky ligands like the β-diketiminate ligands in [(^{Dipp}BDI)Mg]$_2$ can even hinder further reactions, such as dimerisation, due to their high steric demand.

The results show the value of the anthracenide and –diide compounds of the alkaline-earth metals as synthons for their metals in reduction chemistry. This provides an easier access to the metals Mg, Ca, Sr, and Ba as reducing agents in situations where the direct manipulation of the metals is difficult or not feasible. By this way, products can be obtained that cannot be synthesised by using standard reducing agents. The availability of these reagents broadens the scope of available reducing agents in general and offers new opportunities for exploring selective reduction pathways in main-group and transition-metal chemistry.

Data availability

The authors confirm that the data supporting the findings of this study are available within the article and its ESI.†

Author contributions

The conceptualisation (together with M. Scheer) and experimental work were achieved by M. Weber. M. Seidl and C. Riesinger accomplished the solution and refinement of X-ray structural data. Writing of the manuscript of this work was done by M. Weber and L. Adlbert. L. Adlbert performed the DFT calculations. The entire work was supervised, guided, and revised by M. Scheer, who also acquired funding for the project. The final manuscript was reviewed and edited by L. Adlbert and M. Scheer.

Conflicts of interest

There are no conflicts to declare.

Acknowledgements

This work was supported by the Deutsche Forschungsgemeinschaft (DFG) with the project Sche 384/45-1. C. R. is grateful to the Studienstiftung des Deutschen Volkes for his PhD fellowship. Additional references are cited within the ESI.† [46,53–70]

Notes and references

1 B. M. Wolf, C. Stuhl, C. Maichle-Mössmer and R. Anwander, *J. Am. Chem. Soc.*, 2018, **140**, 2373.
2 M. R. Crimmin, A. G. M. Barrett, M. S. Hill, P. B. Hitchcock and P. A. Procopiou, *Organometallics*, 2007, **26**, 2953.
3 K. M. Fromm, *Coord. Chem. Rev.*, 2020, **408**, 213193.
4 B. G. Gowenlock, W. E. Lindsell and B. Singh, *Dalton Trans.*, 1978, 657.
5 D. Naglav, M. R. Buchner, G. Bendt, F. Kraus and S. Schulz, *Angew. Chem., Int. Ed.*, 2016, **55**, 10562.
6 K. Dehnicke and B. Neumüller, *Z. Anorg. Allg. Chem.*, 2008, **634**, 2703.
7 J. T. Boronski, A. E. Crumpton and S. Aldridge, *J. Am. Chem. Soc.*, 2024, **146**, 35208.
8 J. T. Boronski, A. E. Crumpton, A. F. Roper and S. Aldridge, *Nat. Chem.*, 2024, **16**, 1295.
9 J. T. Boronski, A. E. Crumpton, L. L. Wales and S. Aldridge, *Science*, 2023, **380**, 1147.

© 2025 The Author(s). Published by the Royal Society of Chemistry

Open Access Article. Published on 24 July 2025. Downloaded on 1/14/2026 11:15:21 PM. This article is licensed under a Creative Commons Attribution-NonCommercial 3.0 Unported Licence.

10 J. T. Boronski, L. P. Griffin, C. Conder, A. E. Crumpton, L. L. Wales and S. Aldridge, *Chem. Sci.*, 2024, **15**, 15377.
11 B. Rösch, T. X. Gentner, H. Elsen, C. A. Fischer, J. Langer, M. Wiesinger and S. Harder, *Angew. Chem., Int. Ed.*, 2019, **58**, 5396.
12 T. X. Gentner, B. Rösch, K. Thum, J. Langer, G. Ballmann, J. Pahl, W. A. Donaubauer, F. Hampel and S. Harder, *Organometallics*, 2019, **38**, 2485.
13 M. Arrowsmith, M. S. Hill, A. L. Johnson, G. Kociok-Köhn and M. F. Mahon, *Angew. Chem., Int. Ed.*, 2015, **54**, 7882.
14 A. P. Dove, V. C. Gibson, P. Hormnirun, E. L. Marshall, J. A. Segal, A. J. P. White and D. J. Williams, *Dalton Trans.*, 2003, 3088.
15 C. Ruspic and S. Harder, *Inorg. Chem.*, 2007, **46**, 10426.
16 S. Pillai Sarish, A. Jana, H. W. Roesky, T. Schulz, M. John and D. Stalke, *Inorg. Chem.*, 2010, **49**, 3816.
17 V. C. Gibson, J. A. Segal, A. J. P. White and D. J. Williams, *J. Am. Chem. Soc.*, 2000, **122**, 7120.
18 M. Westerhausen, *Dalton Trans.*, 2006, 4755.
19 M. Westerhausen, M. Gärtner, R. Fischer, J. Langer, L. Yu and M. Reiher, *Chem. - Eur. J.*, 2007, **13**, 6292.
20 J. Langer, S. Krieck, H. Görls, G. Kreisel, W. Seidel and M. Westerhausen, *New J. Chem.*, 2010, **34**, 1667.
21 P. K. Freeman and L. L. Hutchinson, *J. Org. Chem.*, 1983, **48**, 879.
22 B. Bogdanović, N. Janke and H.-G. Kinzelmann, *Chem. Ber.*, 1990, **123**, 1507.
23 E. Bartmann, B. Bogdanović, N. Janke, K. Schlichte, B. Spliethoff, J. Treber, U. Westeppe, U. Wilczok and S. Liao, *Chem. Ber.*, 1990, **123**, 1517.
24 B. Bogdanovic, *Acc. Chem. Res.*, 1988, **21**, 261.
25 C. L. Raston and G. Salem, *J. Chem. Soc., Chem. Commun.*, 1984, 1702.
26 W. J. Transue, A. Velian, M. Nava, C. García-Iriepa, M. Temprado and C. C. Cummins, *J. Am. Chem. Soc.*, 2017, **139**, 10822.
27 H. Bönnemann, B. Bogdanivic, R. Brinkmann, N. Egeler, R. Benn, I. Topalovic and K. Seevogel, *Main Group Met. Chem.*, 1990, **13**, 341.
28 O. P. E. Townrow, C. Färber, U. Zenneck and S. Harder, *Angew. Chem., Int. Ed.*, 2024, **63**, e202318428.
29 R. Fischer, M. Gärtner, H. Görls and M. Westerhausen, *Organometallics*, 2006, **25**, 3496.
30 S. Gärtner and N. Korber, in *Zintl Ions: Principles and Recent Developments*, ed. T. F. Fässler, Springer Berlin Heidelberg, Berlin, Heidelberg, 1, 2011, vol. 2, pp. 25–57.
31 W. Dahlmann and H. G. v. Schnering, *Naturwissenschaften*, 1972, **59**, 420.
32 W. Dahlmann and H. G. v. Schnering, *Naturwissenschaften*, 1973, **60**, 429.
33 H. G. von Schnering, M. Wittmann and D. Sommer, *Z. Anorg. Allg. Chem.*, 1984, **510**, 61.
34 B. Eisenmann and U. Rößler, *Z. Anorg. Allg. Chem.*, 2003, **629**, 459.
35 N. Korber and J. Daniels, *Z. Anorg. Allg. Chem.*, 1999, **625**, 189.
36 N. Korber and J. Daniels, *Z. Anorg. Allg. Chem.*, 1996, **622**, 1833.
37 N. Korber and J. Daniels, *Inorg. Chem.*, 1997, **36**, 4906.
38 M. Westerhausen, M. Krofta and A. Pfitzner, *Inorg. Chem.*, 1999, **38**, 598.
39 J. A. Dolyniuk and K. Kovnir, *Crystals*, 2013, **3**, 431.
40 A. Haffner, V. Weippert and D. Johrendt, *Z. Anorg. Allg. Chem.*, 2020, **646**, 120.
41 M. Westerhausen, C. Birg, M. Krofta, P. Mayer, T. Seifert, H. Nöth, A. Pfitzner, T. Nilges and H. J. Deiseroth, *Z. Anorg. Allg. Chem.*, 2000, **626**, 1073.
42 M. B. Cossairt and C. C. Cummins, *Chem.–Eur. J.*, 2010, **16**, 12603.
43 R. Yadav, M. Weber, A. K. Singh, L. Münzfeld, J. Gramüller, R. M. Gschwind, M. Scheer and P. W. Roesky, *Chem.–Eur. J.*, 2021, **27**, 14128.
44 S. Thum, O. P. E. Townrow, J. Langer and S. Harder, *Chem. Sci.*, 2025, **16**, 4528.
45 A. Kracke and C. von Hänisch, *Eur. J. Inorg. Chem.*, 2011, **2011**, 3374.
46 M. Weber, *PhD thesis*, University of Regensburg, 2023.
47 R. F. Winter and W. E. Geiger, *Organometallics*, 1999, **18**, 1827.
48 M. V. Butovskiy, G. Balázs, M. Bodensteiner, E. V. Peresypkina, A. V. Virovets, J. Sutter and M. Scheer, *Angew. Chem., Int. Ed.*, 2013, **52**, 2972.
49 E. Mädl, M. V. Butovskii, G. Balázs, E. V. Peresypkina, A. V. Virovets, M. Seidl and M. Scheer, *Angew. Chem., Int. Ed.*, 2014, **53**, 7643.
50 T. Li, J. Wiecko, N. A. Pushkarevsky, M. T. Gamer, R. Köppe, S. N. Konchenko, M. Scheer and P. W. Roesky, *Angew. Chem., Int. Ed.*, 2011, **50**, 9491.
51 M. Piesch, F. Dielmann, S. Reichl and M. Scheer, *Chem.–Eur. J.*, 2020, **26**, 1518.
52 P. Pyykkö and M. Atsumi, *Chem.–Eur. J.*, 2009, **15**, 186.
53 O. J. Scherer and T. Brück, *Angew. Chem., Int. Ed.*, 1987, **26**, 59.
54 J. Hicks, M. Juckel, A. Paparo, D. Dange and C. Jones, *Organometallics*, 2018, **37**, 4810.
55 G. M. Sheldrick, *Acta Crystallogr., Sect. A*, 2015, **71**, 3.
56 O. V. Dolomanov, L. J. Bourhis, R. J. Gildea, J. A. K. Howard and H. Puschmann, *J. Appl. Crystallogr.*, 2009, **42**, 339.
57 G. M. Sheldrick, *Acta Crystallogr., Sect. C*, 2015, **71**, 3.
58 F. Neese, *Wiley Interdiscip. Rev.:Comput. Mol. Sci.*, 2012, **2**, 73.
59 F. Neese, *Wiley Interdiscip. Rev.:Comput. Mol. Sci.*, 2022, **12**, 1606.
60 F. Neese, F. Wennmohs, U. Becker and C. Riplinger, *J. Chem. Phys.*, 2020, **152**, 224108.
61 F. Neese, *J. Comput. Chem.*, 2023, **44**, 381.
62 A. D. Becke, *Phys. Rev. A*, 1988, **38**, 3098.
63 J. P. Perdew, *Phys. Rev. B: Condens. Matter Mater. Phys.*, 1986, **33**, 8822.
64 F. Weigend, *Phys. Chem. Chem. Phys.*, 2006, **8**, 1057.
65 F. Weigend and R. Ahlrichs, *Phys. Chem. Chem. Phys.*, 2005, **7**, 3297.

Open Access Article. Published on 24 July 2025. Downloaded on 1/14/2026 11:15:21 PM.
This article is licensed under a Creative Commons Attribution-NonCommercial 3.0 Unported Licence.

66 A. D. Becke, *J. Chem. Phys.*, 1993, **98**, 5648.
67 C. Lee, W. Yang and R. G. Parr, *Phys. Rev. B: Condens. Matter Mater. Phys.*, 1988, **37**, 785.
68 E. Caldeweyher, C. Bannwarth and S. Grimme, *J. Chem. Phys.*, 2017, **147**, 34112.
69 E. Caldeweyher, S. Ehlert, A. Hansen, H. Neugebauer, S. Spicher, C. Bannwarth and S. Grimme, *J. Chem. Phys.*, 2019, **150**, 154122.
70 *Chemcraft – Graphical Software For Visualization Of Quantum Chemistry Computations*, **https://www.chemcraftprog.com**.

© 2025 The Author(s). Published by the Royal Society of Chemistry